Optical and microphysical properties of fresh biomass burning aerosol retrieved by Raman lidar, and star-and sun-photometry

L. Alados-Arboledas,[1,2] D. Müller,[3] J. L. Guerrero-Rascado,[1,2,4] F. Navas-Guzmán,[1,2] D. Pérez-Ramírez,[1,2] and F. J. Olmo[1,2]

Received 1 November 2010; revised 22 November 2010; accepted 30 November 2010; published 14 January 2011.

[1] A fresh biomass-burning pollution plume was monitored and characterized in terms of optical and microphysical properties for the first time with a combination of Raman lidar and star- and sun-photometers. Such an instrument combination is highly useful for 24-h monitoring of pollution events. The observations were made at Granada (37.16°N, 3.6°W), Spain. The fresh smoke particles show a rather pronounced accumulation mode and features markedly different from those reported for aged particles. We find lidar ratios around 60–65 sr at 355 nm and 532 nm, and particle effective radii below 0.20 μm. We find low values of the single-scattering albedo of 0.76–0.9 depending on measurement wavelength. The numbers are lower than what have been found for aged, long-range-transported smoke that originated from boreal fires in Canada and Siberia. **Citation:** Alados-Arboledas, L., D. Müller, J. L. Guerrero-Rascado, F. Navas-Guzmán, D. Pérez-Ramírez, and F. J. Olmo (2011), Optical and microphysical properties of fresh biomass burning aerosol retrieved by Raman lidar, and star- and sun-photometry, *Geophys. Res. Lett.*, *38*, L01807, doi:10.1029/2010GL045999.

1. Introduction

[2] Knowledge on smoke particles from fires has attained specific interest in recent years. Smoke is an important source of black carbon which is a key player in atmospheric heating by aerosol particulate pollution. Smoke particles experience medium- to long-range transport and only scarce information is available on particle transformation processes such as particle growth during transcontinental transport. Despite its importance we still have few temporally and vertically resolved observations of smoke (black carbon) optical and microphysical properties. Lidar active remote sensing can close this gap in our understanding of the impact of these aerosols as it provides vertical profiles of aerosol properties. Several authors [*Müller et al.*, 2007, and references therein] present some evidence on particle growth on the basis of height-resolved lidar measurements of forest-fire smoke in the free troposphere. An important gap in these studies however is the observation of fresh smoke plumes near the sources of forest fires in the mid-latitudes. We collected data on a very fresh biomass burning plume with a multiwavelength Raman lidar, a star- and a sun-photometer very close to the source region, i.e., transport time was about 24–36 hours. To our knowledge this is the first time that such observations were carried out. Our study thus contributes to previous studies on aged smoke particle, in particular concerning the first stages of the smoke transport and the vertical variation of some smoke-related parameters. This measurement case furthermore shows the merit of such type of combined instrument observations. Under favorable weather conditions we may observe certain aerosol properties on a 24-hour basis. We may derive a better interpretation on the basis of an analysis of combined data set, which may not be possible if we had only data sets from a single instrument. Furthermore data from one instrument may compensate for a loss of data from another instrument. Section 2 describes the methodology. We present and discuss our results in section 3. We close our contribution with a summary in section 4.

2. Methodology

[3] Data were collected with a Raman lidar, a star- and a sun-photometer, located at the Andalusian Center for Environmental Research located in the city of Granada (Spain, 37.16°N, 3.6°W, 680 m above sea level (a.s.l)). A multiwavelength Raman lidar [*Guerrero-Rascado et al.*, 2009] was used for vertically resolved measurements of particle optical properties of the biomass-burning plume discussed in this contribution. This system provides backscatter coefficients at 355, 532 and 1064 nm, and night-time extinction coefficients at 355 and 532 nm. The aerosol extinction coefficients are derived by the Raman method [*Ansmann and Müller*, 2005]. The full overlap is reached at 970 m above ground. The accuracy of the derived extinction and backscatter profiles is approximately 20% and 15%, respectively. The lidar ratios have maximum errors of 30%. The backscatter coefficient at 1064 nm has been retrieved using Klett's method [*Ansmann and Müller*, 2005] and a methodology described by *Navas-Guzmán et al.* [2010]. Because of calibration problems of our depolarization channel we cannot derive trustworthy particle depolarization ratios.

[4] Aerosol optical depth was measured at night time with the star-photometer *Excalibur*. The star photometer consists basically of a Schmid-Cassegrain telescope and a CCD camera as detector. The instrument has a filter wheel with narrowband filters at 380, 440, 500, 670, 880, 940 and 1020 nm. A detailed description including the data analysis techniques is given by *Pérez-Ramírez et al.* [2008, and the references therein]. At daytime optical depth was measured with an AERONET Cimel radiometer CE-318-4 [*Holben*

[1]Departamento de Física Aplicada, Universidad de Granada, Granada, Spain.
[2]Centro Andaluz de Medio Ambiente, Universidad de Granada, Granada, Spain.
[3]Gwangju Institute of Science and Technology, Kwangju, South Korea.
[4]Évora Geophysics Centre, University of Évora, Évora, Portugal.

0094-8276/11/2010GL045999

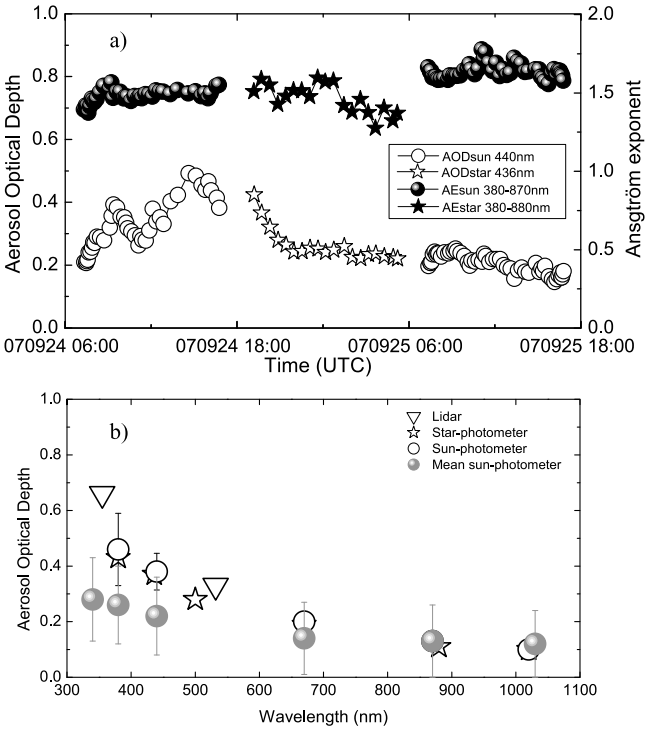

Figure 1. (a) Optical series of aerosol optical depth (AOD in legend) and Ångström exponent (AE) measured with sun- and star-photometer in Granada on 24–25 September 2007. (b) Spectral dependence of aerosol optical depth derived from lidar, sun- and star-photometer measurements. Measurement times are around 16:45 UTC for the sun-photometer, around 19:42 UTC for the star-photometer and between 19:03–20:03 UTC for the lidar. The uncertainty for each data point of aerosol optical depth is <5% for the photometric data and ~10% for the lidar data. The uncertainty of the Ångström exponent is ~20%. The linear correlation coefficient of the fit log AOD vs. log (Ångström exponent) is above 0.99 both for the sun- and star- photometers. Also shown in Figure 1b is the mean spectral optical depth for September 2002–2007 (grey bullets).

et al., 1998]. Only level 1.5 data from AERONET are available for the measurements presented here.

[5] Optical data were used to retrieve microphysical properties by means of an inversion algorithm [*Müller et al.*, 2001; *Ansmann and Müller*, 2005]. For the lidar retrievals, we computed mean backscatter and extinction coefficients for layers of 500-m geometrical depth, respectively. We derive particle size and complex refractive index from which we compute single-scattering albedo with a Mie-scattering algorithm, i.e. we assume that the fresh smoke particles can be described as spheres. We use the same inversion algorithm for the analysis of the optical depth data from sun- and star- photometer. In that case we can only retrieve particle size [*Pahlow et al.*, 2006]. The error bars of the microphysical properties follow from the errors of the input optical data and the uncertainties that are generated by the inversion algorithm. We apply a search grid of complex refractive indices (from 1.3–1.8 in real part and $0i$–$0.1i$ in imaginary part) and particle size parameters (from 10 nm to 5 μm particle radius) which automatically causes approximation errors [*Ansmann and Müller*, 2005]. The uncertainties of single-scattering albedo follow from the uncertainties of the retrieved particle size distributions and the complex refractive indices.

3. Results and Discussion: Case Study From 24 September 2007

[6] In summer 2007, several episodes with large loads (in terms of aerosol optical depth (AOD)) of aerosol particles occurred over Granada [*Guerrero-Rascado et al.*, 2009]. Figure 1 shows that AOD increased on 24 September, with maximum values around sunset, in coincidence with Ångström exponents around 1.3. According to weather maps and our backward-trajectory analysis the synoptic conditions favoured recirculation of air and air mass stagnation below 2 km above sea level (asl). Air flow was from westerly to northerly direction at least up to 5 km asl. Simulations with the NAAPS model predicted the presence of a smoke plumes with particle concentrations up to $4\mu g/m^3$ over Granada and up to 16 $\mu g/m^3$ over the western Iberian Peninsula. Fire MODIS Products indicated a hot spot (at 37.798°N and 3.787°W) around 70 km from Granada in the period from 22–24 September. We used the coordinates of these fires, we know from satellite images when the fires started, and our remote sensing data give us the approximate time when the plume arrived over Granada. In that way we arrive at around 24–36 hours of transport time of the fresh biomass burning particles. AOD again decreases in the early evening. On the basis of our remote sensing data we believe that this decrease was in part caused by inhomogeneities of the smoke plume. We have insufficient information to judge if this decrease in optical depth is also caused by local effects related to the pollution loading in the planetary boundary layer.

[7] Figure 1 shows in more detail the spectral dependence of AOD measured with all three instruments. Optical depth from lidar in the overlap region was computed assuming a constant extinction from the minimum measurement height (around 970 m above ground level) down to the surface. We see good agreement among the data. Due to the measurement principles we do not have overlap of the measurement times of the three instruments. Time-height plots of the range-correct backscatter signals do not indicate any significant change of the plume properties during the measurement period (see caption of Figure 1) that was used for this comparison of spectral dependencies. For comparison Figure 1 shows the mean spectral optical depth for September 2002–2007. The mean Ångström exponent at visible wavelengths for this period is 1.0 ± 0.4.

[8] Figure 2 shows the vertical extension of the aerosol layers on 24 September. The optical profiles show the presence of aerosol particles up to 4 km height asl. About 50% of AOD at 532 nm is contributed by the aerosol layer above 2 km height asl; cf. AOD shown in Figure 1. In the following we discuss our results for the height interval from 2–3.5 km height. In that height range extinction and backscatter coefficients are not negligible (>1 $Mm^{-1}\cdot sr^{-1}$at 532 nm) and lidar misalignment effects are negligible.

[9] The lidar ratios are around 60–65 sr at 355 and 532 nm. For comparison, *Amiridis et al.* [2009] report on biomass burning smoke produced over East Europe. The authors find increasing lidar ratios from 40 sr to nearly 100 sr (at 355 nm) for smoke plumes that increase in age from 7 days to 16 days. Values of 21–67 sr at 355 nm are reported by *Müller et al.*

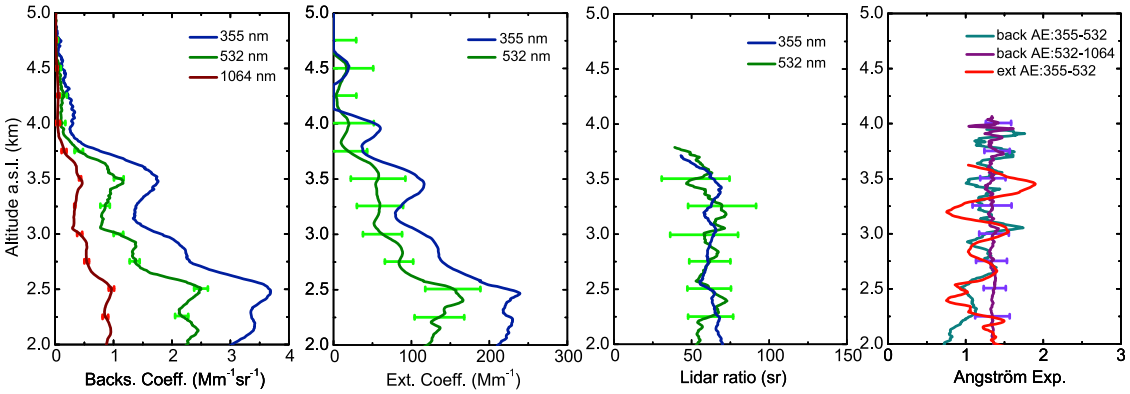

Figure 2. Mean profiles of aerosol optical properties (extinction coefficients, backscatter coefficients, lidar ratios, and backscatter-related and extinction-related Ångström exponents) for the measurement from 19:03 to 20:03 UTC on 24 September 2007. Error bars denote one-standard deviation.

[2005, Table 1] for biomass burning smoke advected from North America and Siberia to Germany after up to 2.5 weeks of transport time. Lidar ratios of 40 sr and 65 sr at 355 nm and 532 nm, respectively, were observed for Siberian forest fire smoke over Japan after approximately 4 days of transport time [*Murayama et al.*, 2004]. Lidar ratios depend on size, shape and chemical composition of the particles, which in turn depend on kind of burned biomass, intensity of the fire, and many additional factors. The complex influence of various parameters may be the reason that there is no clear pattern of change of lidar ratio, for instance at 355 nm with age of the smoke plume. More interestingly the ratio of the lidar ratios (value at 355 nm to value at 532 nm) for the case of fresh smoke presented here is around unity, whereas the ratio for aged fire smoke is less than one [*Murayama et al.*, 2004; *Müller et al.*, 2005]. This ratio difference puts additional weight on the assumption that we observe comparably fresh smoke over Granada. Up to now we observed ratios less than unity for aged, long-range-transported smoke.

[10] Backscatter and extinction related Ångström exponents are 1–1.5 (wavelength pair 355/532 nm). These numbers indicate that particles in the accumulation mode are dominant, which is a typical feature of smoke particles from fires. For comparison, aged smoke particles (after long-range transport of several days) show extinction-related-Ångström exponents close to zero and backscatter-related Ångström exponents of approximately one [*Wandinger et al.*, 2002; *Müller et al.*, 2005].

[11] Table 1 presents effective radius (r_{eff}), real (m_{real}) and imaginary (m_{imag}) part of the complex refractive index, and single scattering albedo (ω) for several height layers. We also show column-integrated values of effective radius obtained from the inversion of optical depth measured with star- and sun-photometer. Table 1 shows excellent agreement of effective radius derived from the active and passive remote sensing data. The columnar-integrated effective radii tend to be slightly higher than those retrieved from lidar although all retrieved radii are below 0.2 μm. At our station, typical values of effective radius for total, fine and coarse mode are 0.40 ± 0.17 μm, 0.13 ± 0.02 μm, and 2.2 ± 0.4 μm, respectively. The numbers describe the period from 2004 to 2008 (AERONET level 2 data).

[12] Effective radii found in this study are lower than those obtained for long-range transport of aged Siberian forest fire smoke over Japan, i.e., 0.22 ± 0.04 μm [*Murayama et al.*, 2004]. An effective radius of around 0.25 μm was determined during LACE98 for a long-range transported biomass burning plume that originated from forest fires in northwestern Canada [*Wandinger et al.*, 2002]. *O'Neill et al.* [2002] presents optical and microphysical parameters of fire smoke observed with sunphotometer close to the source region in Canada. These authors report on effective radii around 0.14 μm. Our values for particle effective radius fall within this broad range of numbers. *Müller et al.* [2007] present a study of particle growth during long-range transport of forest-fire smoke from Raman lidar and sunphotometry observations. The authors find a parameterization which describes particle growth with transport time. Interestingly our results on particle size fall onto this particle growth curve.

[13] Physical and chemical processes like particle coagulation and particle-size specific sedimentation, as well as gas-to-particle condensation processes may be responsible

Table 1. Mean Aerosol Microphysical Properties Derived From the Lidar Profiles, and Columnar-Integrated Microphysical Properties[a]

In	Range (km)	Ångstöm 355/532 nm	r_{eff} (μm)	m_{real}	m_{imag}	ω_{355}	ω_{532}	ω_{1064}
RL	2.0–2.5	1.16 ± 0.22	0.17 ± 0.06	1.49 ± 0.12	0.02 ± 0.02	0.76 ± 0.14	0.80 ± 0.13	0.86 ± 0.11
	2.5–3.0	1.20 ± 0.16	0.15 ± 0.05	1.53 ± 0.13	0.02 ± 0.02	0.78 ± 0.13	0.83 ± 0.12	0.87 ± 0.11
	3.0–3.5	1.3 ± 0.4	0.13 ± 0.03	1.53 ± 0.14	0.02 ± 0.02	0.83 ± 0.10	0.87 ± 0.08	0.90 ± 0.07
StP	column	1.61 ± 0.10	0.19 ± 0.05	-	-	-	-	-
SPM	column	1.34 ± 0.08	0.20 ± 0.05	-	-	-	-	-

[a]Shown are effective radius (r_{eff}), real (m_{real}) and imaginary (m_{imag}) part of the complex refractive index and single-scattering albedo at 355, 532 and 1064 nm (ω_{355}, ω_{532}, ω_{1064}). Also shown is the Ångström exponent from the extinction measurements with lidar (355/532 nm wavelength pair) and from optical depth measured with sunphotometer (380/500 nm wavelength pair). The lidar results hold for the measurement from 19:03 to 20:03 UTC on 24 September 2007. Results for star photometer and sunphotometer hold for the measurement around 19:42 UTC and 16:45 UTC, respectively.

for the observed particle size. Also the specific properties of the burnt material and the burning processes (flaming versus smoldering fire) may generate different particle sizes at the source of the fires. However, we know too little of this processes and the causes of particle size modification during atmospheric transport, and thus an explanation on why particle size reported here fits to this parameterization must be left open for future studies.

[14] Table 1 presents the complex refractive index. The real part varies between 1.49–1.53. The imaginary part is $0.02i$. Both real and imaginary parts are quite constant with altitude, given the comparably large uncertainties. For comparison highly absorbing smoke particles have been reported in previous studies. A summary for different regions on the globe (South America, South India) is given by *Müller et al.* [2005]. Real parts range from 1.5 to 1.66 at visible wavelengths. Imaginary parts cover values from $0.01i$–$0.07i$. The complex refractive indices reported in these references do not show a clear pattern of change of imaginary part with transport time. Crucial information like air mass transport times, as well as kind of burnt material and type of fires is missing. For this reason any further interpretation of our results regarding change of particle light-absorption with age of particles cannot be done.

[15] The single scattering albedoes slightly increases with altitude, Table 1. The values vary between 0.76 and 0.90 with a slightly positive spectral dependence. These values are in the range of those encountered in the literature. *Murayama et al.* [2004] report a single scattering albedo of 0.95 ± 0.06 at 532 nm around the peak of a Siberian forest fire smoke event over Japan. *O'Neill et al.* [2002] retrieved single scattering albedo in the range 0.97 to 0.99, 32 km from the biomass burning aerosol sources. *Alados-Arboledas et al.* [2007] obtained single scattering albedoes ranging from 0.80–0.87 (440–1020 nm) for a lofted smoke plume monitored at a high mountain station with sunphotometer. *Wandinger et al.* [2002] found single scattering albedoes of 0.76 ± 0.06 and 0.81 ± 0.05 at 355 and 532 nm, respectively, for transport of forest-fire smoke from western Canada. *Eck et al.* [2009] find values above 0.95 at visible wavelengths for smoke from smoldering forest fires observed with sunphotometer in Alaska. *Reid et al.* [2005] report that single-scattering albedo of biomass-burning aerosols typically decreases with increasing measurement wavelength. We are cautious though with a respective interpretation of our results for single-scattering albedo. The inversion procedure applied to the lidar profiles does not consider any spectral dependence of the refractive index. Thus, the spectral dependence of single-scattering albedo is only driven by the effect of the particle size distribution.

4. Summary

[16] We present a first comprehensive study of optical and microphysical properties of particulate pollution that describes rather fresh biomass burning aerosol. The observations were made with a combination of active, Raman lidar, and passive, star- and sunphotometry, remote sensing instrumentation. Our results allow us to extend previous studies on ageing of biomass burning aerosols due to the extremely short transport time of this event. The lidar observations on 24 September 2007 show that up to 50% of optical depth at 532 nm was contributed by this fresh smoke layer. Ångström exponents for the wavelength range from 355 to 532 nm were up to 1.3 and thus on average larger than what is usually observed for aged smoke particles. Column-averaged Ångström exponents derived from sunphotometer measurements were rather close to those values, both, before and after the night time Raman lidar observations. Star-photometer measurements, in coincidence with the lidar observations, provide similar results. The column-averaged lidar ratios range between 60–65 sr at 355 nm and 532 nm, respectively. In contrast, aged long-range-transported smoke particles show lidar ratios which are larger at 532 nm compared to the values at 355 nm. There is reasonable agreement for the microphysical parameters, i.e., effective radius and the complex refractive index. The particle radius of the fresh fire smoke particles is below 0.2 μm, which is less than the typical values found for long-range transported, aged smoke particles in boreal areas of the Northern Hemisphere. The imaginary part varies around $0.02i$, indicating comparably strong light-absorption of the smoke particles. The single scattering albedo ranges between 0.76 and 0.90 depending on wavelength.

[17] **Acknowledgments.** This work is supported by Spanish Ministry of Education and Science under the Acciones Complementarias CGL-2006-27108-E/CLI (DAMOCLES Aerosol Scientific Thematic Network); and CGL2008-01330-E/CLI and CGL2007-28871-E/CLI (Spanish Lidar Network); project CGL2010-18782 and CSD2007-00067 of the Spanish Ministry of Education; project P08-RNM-3568 and P10-RNM-6299 of the Autonomous Government of Andalusia, and by the EARLINET-ASOS project (EU Coordination Action, contract 025991 (RICA)). The authors express gratitude to the NOAA Air Resources Laboratory (ARL) and Naval Research Laboratory for the HYSPLIT transport and dispersion model and the NAAPS aerosol maps.

References

Alados-Arboledas, L., J. L. Guerrero-Rascado, H. Lyamani, F. Navas-Guzmán, and F. J. Olmo (2007), Characterization of the atmospheric aerosol by combination of Lidar and sun-photometry, *Proc. SPIE*, *6750*, 67500J, doi:10.1117/12.737557.

Amiridis, V., D. S. Balis, E. Giannakaki, A. Stohl, S. Kazadzis, M. E. Koukouli, and P. Zanis (2009), Optical characteristics of biomass burning aerosols over Southeastern Europe determined from UV-Raman lidar measurements, *Atmos. Chem. Phys.*, *9*, 2431–2440, doi:10.5194/acp-9-2431-2009.

Ansmann, A., and D. Müller (2005), Lidar and atmospheric aerosol particles, in *Lidar. Range-Resolved Optical Remote Sensing of the Atmosphere*, edited by C. Weitkamp, pp. 105–114, Springer, Singapore.

Eck, T. F., et al. (2009), Optical properties of boreal region biomass burning aerosols in central Alaska and seasonal variation of aerosol optical depth at an Arctic coastal site, *J. Geophys. Res.*, *114*, D11201, doi:10.1029/2008JD010870.

Guerrero-Rascado, J. L., F. J. Olmo, I. Avilés-Rodríguez, F. Navas-Guzmán, D. Pérez-Ramírez, H. Lyamani, and L. Alados-Arboledas (2009), Extreme Saharan dust event over the southern Iberian Peninsula in September 2007: Active and passive remote sensing from surface and satellite, *Atmos. Chem. Phys.*, *9*, 8453–8469, doi:10.5194/acp-9-8453-2009.

Holben, B. N., et al. (1998), AERONET—A federated instrument network and data archieve for aerosol characterization, *Remote Sens. Environ.*, *66*, 1–16, doi:10.1016/S0034-4257(98)00031-5.

Müller, D., U. Wandinger, D. Althausen, and M. Fiebig (2001), Comprehensive particle characterization from three-wavelength Raman lidar observations: Case study, *Appl. Opt.*, *40*, 4863–4869, doi:10.1364/AO.40.004863.

Müller, D., I. Mattis, U. Wandinger, A. Ansmann, D. Althausen, and A. Stohl (2005), Raman lidar observations of aged Siberian and Canadian forest fire smoke in the free troposphere over Germany in 2003: Microphysical particle characterization, *J. Geophys. Res.*, *110*, D17201, doi:10.1029/2004JD005756.

Müller, D., I. Mattis, A. Ansmann, U. Wandinger, C. Ritter, and D. Kaiser (2007), Multiwavelength Raman lidar observations of particle growth

during long-range transport of forest-fire smoke in the free troposphere, *Geophys. Res. Lett.*, *34*, L05803, doi:10.1029/2006GL027936.

Murayama, T., D. Müller, K. Wada, A. Shimizu, M. Sekigushi, and T. Tsukamato (2004), Characterization of Asian dust and Siberian smoke with multi-wavelength Raman lidar over Tokyo, Japan in spring 2003, *Geophys. Res. Lett.*, *31*, L23103, doi:10.1029/2004GL021105.

Navas-Guzmán, F., J. L. Guerrero-Rascado, J. A. Bravo-Aranda, and L. Alados-Arboledas (2010), Calibration of 1064nm-backscatter profiles with a multiwavelength Raman Lidar, *Rom. J. Phys.*, in press.

O'Neill, N. T., T. F. Eck, B. N. Holben, A. Smirnov, A. Royer, and Z. Li (2002), Optical properties of boreal forest fire smoke derived from Sun photometry, *J. Geophys. Res.*, *107*(D11), 4125, doi:10.1029/2001JD000877.

Pahlow, M., D. Müller, M. Tesche, H. Eichler, G. Feingold, W. E. Eberhard, and Y. F. Cheng (2006), Retrieval of aerosol properties from combined multiwavelength lidar and sunphotometer measurements, *Appl. Opt.*, *45*, 7429–7442, doi:10.1364/AO.45.007429.

Pérez-Ramírez, D., J. Aceituno, B. Ruiz, F. J. Olmo, and L. Alados-Arboledas (2008), Development and calibration of a star photometer to measure the aerosol optical depth: Smoke observations at a high mountain site, *Atmos. Environ.*, *42*(11), doi:10.1016/j.atmosenv.2007.06.009.

Reid, J. S., T. F. Eck, S. A. Christopher, R. Koppmann, O. Dubovik, D. P. Eleuterio, B. N. Holben, E. A. Reid, and J. Zhang (2005), A review of biomass burning emissions: Part III. Intensive optical properties of biomass burning particles, *Atmos. Chem. Phys.*, *5*, 827–849, doi:10.5194/acp-5-827-2005.

Wandinger, U., et al. (2002), Optical and microphysical characterization of biomass-burning and industrial-pollution aerosols from multiwavelength lidar and aircraft measurements, *J. Geophys. Res.*, *107*(D21), 8125, doi:10.1029/2000JD000202.

L. Alados-Arboledas, J. L. Guerrero-Rascado, F. Navas-Guzmán, F. J. Olmo, and D. Pérez-Ramírez, Departamento de Física Aplicada, Universidad de Granada, E-18071 Granada, Spain. (alados@ugr.es)

D. Müller, Gwangju Institute of Science and Technology, 1 Cheomdan-Gwagiro (Oryong-dong), Buk-Gu, Kwangju 500-712, South Korea.